The skewness of elliptic flow fluctuations

Giuliano Giacalone,[1] Li Yan,[1] Jacquelyn Noronha-Hostler,[2] and Jean-Yves Ollitrault[1]

[1] *Institut de physique théorique, Université Paris Saclay, CNRS, CEA, F-91191 Gif-sur-Yvette, France*
[2] *Department of Physics, University of Houston, Houston TX 77204, USA*

(Dated: August 8, 2016)

Using event-by-event hydrodynamic calculations, we find that the fluctuations of the elliptic flow (v_2) in the reaction plane have a negative skew. Comparing the skewness of the v_2 fluctuations to that of the initial eccentricity fluctuations, we show that skewness is the main effect that separates higher-order cumulants. Furthermore, negative skew corresponds to the hierarchy $v_2\{4\} > v_2\{6\}$ observed in Pb+Pb collisions at the LHC. We describe how the skewness can be measured experimentally and show that hydrodynamics naturally reproduces its magnitude and centrality dependence.

I. INTRODUCTION

Elliptic flow, v_2, is one of the key observables of ultra-relativistic heavy-ion collisions at RHIC [1] and LHC [2]. Its large magnitude suggests that the strongly-coupled system formed in these collisions behaves collectively as a fluid [3]. However, quantitative comparison between hydrodynamic calculations and experimental data is hindered by the poor knowledge of the early collision dynamics and of the transport properties of the quark-gluon plasma [4]. Therefore, it is essential to identify *qualitative* features predicted by hydrodynamics which can be tested against experimental data.

A crucial step in our understanding of collective motion has been the recognition that v_2 fluctuates event to event [5, 6]. Elliptic flow fluctuations are quantitatively probed by the cumulants [7] $v_2\{k\}$, with $k = 2, 4, 6, 8$ [8]. One typically observes $v_2\{2\} > v_2\{4\}$ and almost degenerate values for $v_2\{4\}$, $v_2\{6\}$, $v_2\{8\}$, corresponding to Gaussian fluctuations of v_2 [9]. A fine splitting (at the percent level) between $v_2\{4\}$ and $v_2\{6\}$ is however observed above 40% centrality [10]. This splitting is a signature of non-Gaussian fluctuations. Non-Gaussianity is in fact expected in hydrodynamics because v_2 is proportional to the corresponding spatial anisotropy (denoted by ε_2) of the initial density profile [11], and the fluctuations of ε_2 present generic non-Gaussian properties [12, 13].

In this article, we identify the main source of non-Gaussian fluctuations with the skewness of elliptic flow fluctuations in the reaction plane. We compute the skewness in event-by-event hydrodynamics (Sec. II) and compare it with the skewness of eccentricity fluctuations. We then show (Sec. III), by means of an expansion in powers of the fluctuations, that skewness is the leading contribution to the fine structure of higher-order cumulants. We compare experimental data with hydrodynamic calculations. In Sec. IV, we derive a general formula relating the standardized skewness to the first three cumulants, $v_2\{2\}$, $v_2\{4\}$ and $v_2\{6\}$.

II. SKEWNESS IN EVENT-BY-EVENT HYDRODYNAMICS

In the flow picture [14], particles are emitted independently in each collision with an azimuthal probability distribution $P(\varphi)$ that fluctuates event to event. We choose a coordinate frame where $\varphi = 0$ is the direction of the reaction plane. Elliptic flow is defined as the 2nd Fourier coefficient of $P(\varphi)$, which has cosine and sine components:

$$v_x \equiv \frac{1}{2\pi}\int_0^{2\pi} P(\varphi)\cos 2\varphi\, d\varphi,$$
$$v_y \equiv \frac{1}{2\pi}\int_0^{2\pi} P(\varphi)\sin 2\varphi\, d\varphi. \tag{1}$$

Elliptic flow is a two-dimensional vector, $\mathbf{v}_2 = v_x\mathbf{e}_x + v_y\mathbf{e}_y$. Using the standard terminology, we denote by v_2 the magnitude of $\mathbf{v}_2$, i.e. $v_2 \equiv \sqrt{v_x^2 + v_y^2}$.

Since the probability distribution $P(\varphi)$ fluctuates event to event, the projections v_x and v_y are fluctuating quantities. In hydrodynamics, these fluctuations result mainly from the fluctuations of the initial energy density profile and are due to the probabilistic nature of the positions of the nucleons within nuclei at the time of impact [5, 6]. $\mathbf{v}_2$ is to a good approximation [11, 15] proportional to the initial eccentricity $\boldsymbol{\varepsilon}_2 = (\varepsilon_x, \varepsilon_y)$, which is defined by [16]:

$$\varepsilon_x \equiv -\frac{\int \rho(r,\phi) r^2 \cos 2\phi\, r dr d\phi}{\int \rho(r,\phi) r^2\, r dr d\phi},$$
$$\varepsilon_y \equiv -\frac{\int \rho(r,\phi) r^2 \sin 2\phi\, r dr d\phi}{\int \rho(r,\phi) r^2\, r dr d\phi}, \tag{2}$$

where $\rho(r,\phi)$ is the energy density deposited in the transverse plane shortly after the collision, in a centered polar coordinate system.

We model elliptic flow fluctuations by carrying out event-by-event hydrodynamic calculations of Pb+Pb collisions at 2.76 TeV, with initial conditions given by the Monte Carlo Glauber model [17–19]. Our setup is the same as in Ref. [20]: The shear viscosity over entropy ratio is $\eta/s = 0.08$ [21] within the viscous relativistic hydrodynamical code v-USPhydro [22–24] that passes known

analytical solutions [25], and v_x and v_y are calculated using Eq. (1) at freeze-out [26] for pions in the transverse momentum range $0.2 < p_t < 3$ GeV/c.

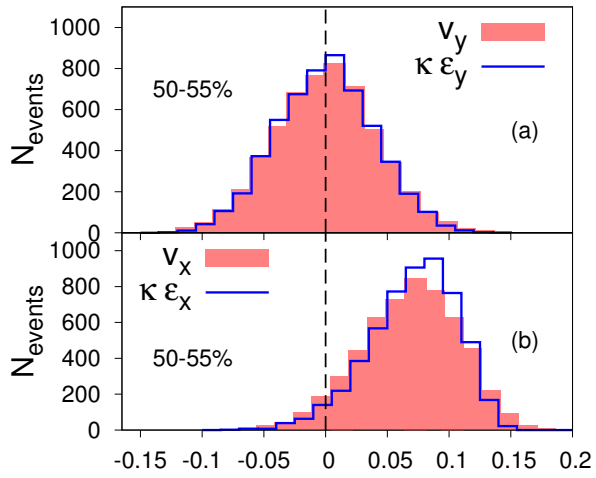

FIG. 1. (Color online) Shaded areas: Histograms of the distribution of v_y (a) and v_x (b) for Pb+Pb collisions in the 50-55% centrality range. 5509 events were generated. Full lines: Histograms of the distributions of ε_y (a) and ε_x (b), rescaled by a response coefficient $\kappa = 0.21$.

Figure 1 displays the histograms of the distributions of v_y (a) and v_x (b) in the 50-55% centrality bin. We choose this rather peripheral centrality range as an illustration because elliptic flow is close to its maximum value [2] and presents large fluctuations. Values of v_x are positive for most events, corresponding to elliptic flow in the reaction plane [27]. We denote by $\bar{v}_2$ its mean value

$$\bar{v}_2 \equiv \langle v_x \rangle, \tag{3}$$

where angular brackets denote an average over events in a centrality class. Note that $\bar{v}_2$ is smaller than the mean elliptic flow $\langle v_2 \rangle = \langle \sqrt{v_x^2 + v_y^2} \rangle$. The distribution of v_y is centered at 0 because parity conservation and symmetry with respect to the reaction plane imply that the probability distribution of (v_x, v_y) is symmetric under $v_y \to -v_y$. The magnitude of the fluctuations is characterized by the variances of v_x and v_y:

$$\begin{aligned} \sigma_x^2 &= \langle (v_x - \bar{v}_2)^2 \rangle = \langle v_x^2 \rangle - \langle v_x \rangle^2, \\ \sigma_y^2 &= \langle v_y^2 \rangle. \end{aligned} \tag{4}$$

For small fluctuations, the fluctuations of v_x correspond to the fluctuations of the flow magnitude, while the fluctuations of v_y correspond to the fluctuations of the flow angle. The so-called Bessel-Gaussian distribution [9] is obtained by assuming that the distribution of $\mathbf{v}_2$ is a two-dimensional Gaussian whose fluctuations are isotropic, i.e. $\sigma_x = \sigma_y$. While this is typically a good approximation for central and mid-central collisions, it becomes worse as the centrality percentile increases. In particular, Fig. 1 shows that σ_y is slightly larger than σ_x, a general feature which can be traced back to the fluctuations of the initial eccentricity [12]. The relative difference between σ_y and σ_x is in the fourth Fourier harmonic [28] and, therefore, scales like $(\bar{v}_2)^2$.

The distributions of ε_x and ε_y are also displayed in Fig. 1, rescaled by a coefficient κ, so that the mean value of ε_x matches that of the v_x distribution. If $\mathbf{v}_2$ was linearly proportional to $\boldsymbol{\varepsilon}_2$, then the two distributions would be identical. The distribution of v_x is somewhat broader than that of ε_x, mostly because of a cubic response term, which is expected to have a sizable contribution at large centrality [20].

One sees in Fig. 1 (b) that the distributions of v_x and ε_x are not symmetric with respect to their maximums: they present negative skew. The skewness of the distribution of ε_x results from the condition $\varepsilon_x \leq 1$, which acts as a right cutoff [12]. Skewness is typically characterized by the third moment of the fluctuations. The symmetry $v_y \to -v_y$ allows for two non trivial moments to order 3:

$$\begin{aligned} s_1 &\equiv \langle (v_x - \bar{v}_2)^3 \rangle, \\ s_2 &\equiv \langle (v_x - \bar{v}_2) v_y^2 \rangle. \end{aligned} \tag{5}$$

The negative skew in Fig. 1 (b) corresponds to $s_1 < 0$. For dimensional reasons, a standardized skewness is usually employed, which is defined as

$$\gamma_1 \equiv \frac{s_1}{\sigma_x^3}. \tag{6}$$

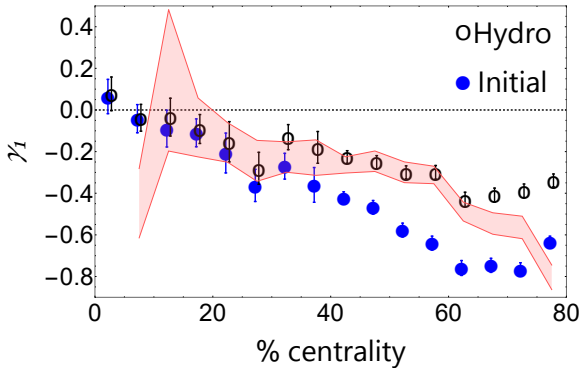

FIG. 2. (Color online) Standardized skewness of elliptic flow fluctuations (open circles) and of initial eccentricity fluctuations (full circles) from hydrodynamic calculations, as a function of centrality percentile, for Pb+Pb collisions at 2.76 TeV. Symbols have been slightly shifted horizontally for the sake of readability. The shaded band displays the value of γ_1 estimated from the cumulants of v_2, as defined by Eq. (16).

Figure 2 displays the standardized skewness γ_1 calculated in hydrodynamics as a function of the collision centrality. It is negative above 20% centrality and its absolute magnitude increases as a function of centrality percentile. This increase results from two effects: first, γ_1 vanishes by symmetry for central collisions and is typically proportional to $\bar{v}_2$; second, it is a first-order correction to the central limit and is, therefore, inversely

proportional to the square root of the system size [13]. Figure 2 also displays the standardized skewness of the ε_x fluctuations, which, as we pointed out before, would be identical to that of the v_x fluctuations if $\mathbf{v}_2$ was exactly linearly proportional to $\boldsymbol{\varepsilon}_2$. We observe that the skewness calculated from $\mathbf{v}_2$ becomes smaller in absolute value than the initial skewness calculated from $\boldsymbol{\varepsilon}_2$ as the centrality percentile increases. Hence, the hydrodynamical evolution washes out part of the initial skewness. This effect is mostly due to the cubic response of the system, which increases σ_x [20].

Eqs. (3)-(5) are the first order terms in a cumulant expansion of the flow fluctuations. The formalism of generating functions provides a compact formulation for the cumulant expansion. The Fourier-Laplace transform of the distribution of $\mathbf{v_2}$ is $\langle e^{\mathbf{k}\cdot\mathbf{v}_2}\rangle$, where $\mathbf{k} \equiv k_x\mathbf{e}_x + k_y\mathbf{e}_y$ is a two-dimensional vector. The generating function of the cumulants is its logarithm, $\ln\langle e^{\mathbf{k}\cdot\mathbf{v}_2}\rangle$. By expanding it up to order 3 in $\mathbf{k}$, one obtains

$$\ln\langle e^{\mathbf{k}\cdot\mathbf{v}_2}\rangle = k_x\bar{v}_2 + \frac{k_x^2}{2}\sigma_x^2 + \frac{k_y^2}{2}\sigma_y^2 + \frac{k_x^3}{6}s_1 + \frac{k_x k_y^2}{2}s_2, \quad (7)$$

where $\bar{v}_2$, σ_x, σ_y, s_1 and s_2 are given by Eqs. (3-5).

III. THE FINE STRUCTURE OF HIGHER-ORDER CUMULANTS

The direction of the reaction plane is not known experimentally. Therefore, the skewness of the v_x fluctuations defined in Eq. (6) cannot be measured directly. More specifically, there is no simple way of extracting it from the probability distribution of the flow magnitude, v_2 [29]. In this section, we show how one can relate the skewness to quantities which are measured experimentally, specifically, the cumulants of the distribution of v_2.

Experimental observables are measured in the laboratory frame where the orientation of the reaction plane has a flat distribution. The cumulants of the distribution of v_2, as measured in experiments[2, 8, 30–32], are defined in this frame [7, 33]. Their generating function is given by the left-hand side of Eq. (7), with the only difference that one averages over the orientation of the reaction plane before taking the logarithm. One, therefore, exponentiates Eq. (7), substitutes $k_x = k\cos\varphi$ and $k_y = k\sin\varphi$, averages over φ and finally takes the logarithm:

$$\ln G(k) \equiv \ln\left(\int_0^{2\pi}\frac{d\varphi}{2\pi}\langle \mathrm{e}^{\mathbf{k}\cdot\mathbf{v}_2}\rangle\right). \quad (8)$$

The $2n$-th order cumulant, $v_2\{2n\}$, is eventually given by the $2n$-th order term of the Taylor expansion of $\ln G(k)$ computed at $k = 0$[1]. More specifically [7]:

$$\left.\frac{d^{2n}}{dk^{2n}}\ln I_0(kv_2\{2n\})\right|_{k=0} \equiv \left.\frac{d^{2n}}{dk^{2n}}\ln G(k)\right|_{k=0}. \quad (9)$$

In the simple case of Bessel-Gaussian fluctuations, $s_1 = s_2 = 0$ and $\sigma_y = \sigma_x$. Inserting Eq. (7) into Eq. (8) one obtains

$$\ln G(k) = \ln I_0(k\bar{v}_2) + \frac{k^2\sigma_x^2}{2} \quad (10)$$

and Eq. (9) yields

$$\begin{aligned} v_2\{2\} &= \sqrt{(\bar{v}_2)^2 + 2\sigma_x^2}, \\ v_2\{4\} = v_2\{6\} &= \cdots = \bar{v}_2. \end{aligned} \quad (11)$$

Therefore, the cumulants of order $n \geq 4$ are identical to the mean elliptic flow in the reaction plane [9].

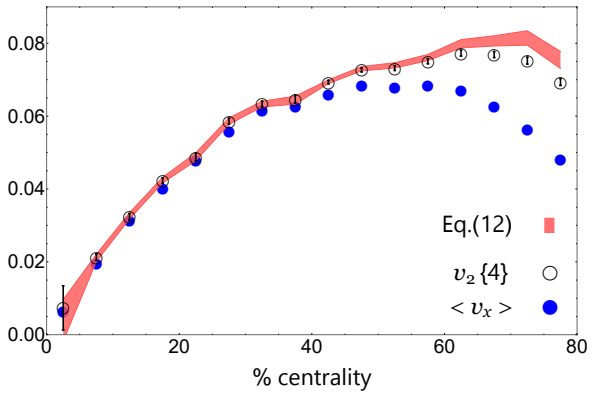

FIG. 3. (Color online) Open symbols: $v_2\{4\}$ versus centrality in event-by-event hydrodynamics. Full symbols: mean elliptic flow in the reaction plane $\langle v_x\rangle = \bar{v}_2$. Shaded band: right-hand side of Eq. (12) for $v_2\{4\}$, corresponding to the leading non-Gaussian corrections.

In event-by-event hydrodynamics, the direction of the reaction plane is known and one can compute both $v_2\{4\}$ [34–37] and $\bar{v}_2$. Figure 3 shows their dependence on the centrality percentile where they are compatible up to 40% centrality. For peripheral collisions, $v_2\{4\}$ becomes significantly larger than $\bar{v}_2$, which means that the Bessel-Gaussian ansatz fails [34]. This failure can be attributed either to the asymmetry of the fluctuations, $\sigma_x \neq \sigma_y$, or to non-Gaussian fluctuations. Both these features are expected in hydrodynamics, as shown in Sec. II. Expanding the generating function in powers of the fluctuations and keeping only the leading order terms in $\sigma_y^2 - \sigma_x^2$, s_1 and s_2, we obtain:

$$v_2\{2\} = \sqrt{(\bar{v}_2)^2 + \sigma_x^2 + \sigma_y^2},$$

[1] In the Taylor expansion we consider only terms of order $2n$ because $I_0(k)$ is even.

$$v_2\{4\} \simeq \bar{v}_2 + \frac{\sigma_y^2 - \sigma_x^2}{2\bar{v}_2} - \frac{s_1 + s_2}{(\bar{v}_2)^2},$$
$$v_2\{6\} \simeq \bar{v}_2 + \frac{\sigma_y^2 - \sigma_x^2}{2\bar{v}_2} - \frac{\frac{2}{3}s_1 + s_2}{(\bar{v}_2)^2},$$
$$v_2\{8\} \simeq \bar{v}_2 + \frac{\sigma_y^2 - \sigma_x^2}{2\bar{v}_2} - \frac{\frac{7}{11}s_1 + s_2}{(\bar{v}_2)^2}, \qquad (12)$$

When these corrections are added, higher-order cumulants are no longer equal to $\bar{v}_2$. The shaded band in Fig. 3 corresponds to the right-hand side of the second line of Eq. (12), where all terms are calculated in hydrodynamics. Agreement with the left-hand side is excellent for all centralities. The term proportional to the asymmetry of the fluctuations, $\sigma_y^2 - \sigma_x^2$, turns out to be negligible: The leading correction is the term proportional to $s_1 + s_2$, due to the non-Gaussianity of the fluctuations.

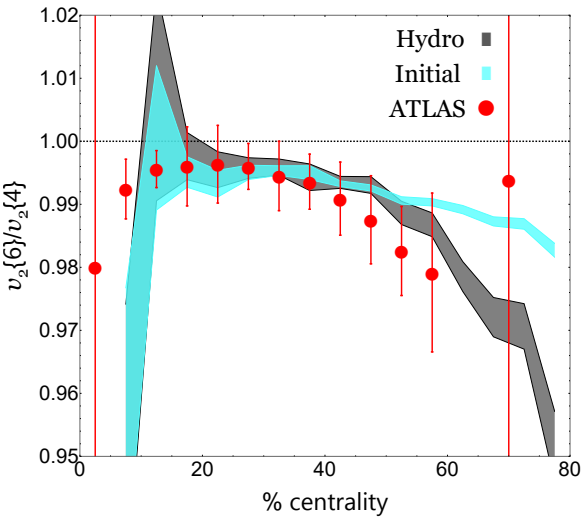

FIG. 4. (Color online) Symbols: ATLAS data for $v_2\{6\}/v_2\{4\}$ versus centrality [8]. Error bars take into account the strong correlation between $v_2\{6\}$ and $v_2\{4\}$ [7]. Dark shaded band: hydrodynamic calculations. Light shaded band: $\varepsilon_2\{6\}/\varepsilon_2\{4\}$.

Non-Gaussian fluctuations not only increase the value of $v_2\{4\}$: They also induce a splitting between $v_2\{4\}$, $v_2\{6\}$ and $v_2\{8\}$. Subtracting the second and third line of Eq. (12), one obtains:

$$v_2\{4\} - v_2\{6\} = -\frac{s_1}{3(\bar{v}_2)^2}. \qquad (13)$$

The splitting is solely due to the coefficient s_1, corresponding to the skewness of elliptic flow fluctuations in the reaction plane.[2] Figure 4 displays ATLAS data [8] for $v_2\{6\}/v_2\{4\}$ versus centrality for Pb+Pb collisions at 2.76 TeV. $v_2\{4\}$ and $v_2\{6\}$ are very close to one another for all centralities, but a fine structure is however seen at the percent level above 40% centrality, where $v_2\{4\}$ is larger than $v_2\{6\}$. According to Eq. (13), this implies that $s_1 < 0$, in line with our expectation from the hydrodynamic calculations presented in Sec. II. We carry out a more quantitative comparison by numerical calculations of $v_2\{6\}/v_2\{4\}$ in hydrodynamics. The result is displayed as a dark shaded band in Fig. 4. It is compatible with experimental data within error bars. Precise figures depend on the model of initial conditions, but Fig. 4 shows that hydrodynamics naturally captures the skewness of the v_2 fluctuations, hence the splitting between $v_2\{4\}$ and $v_2\{6\}$. In our hydrodynamic calculation, the ratio $v_2\{6\}/v_2\{4\}$ coincides with the corresponding ratio for initial eccentricities, $\varepsilon_2\{6\}/\varepsilon_2\{4\}$, up to 60% centrality[3]. Unlike the ratio $v_2\{4\}/v_2\{2\}$ [20], the fine structure of higher-order cumulants is essentially unaffected by the cubic response and directly reflects the ratio $\varepsilon_2\{6\}/\varepsilon_2\{4\}$ provided by the model of initial conditions.

Eq. (12) also gives the following universal prediction for the small splitting between $v_2\{6\}$ and $v_2\{8\}$:

$$v_2\{6\} - v_2\{8\} = \frac{1}{11}(v_2\{4\} - v_2\{6\}). \qquad (14)$$

The number of events in our hydrodynamic calculation is too small to test this relation. We have, therefore, tested it on the cumulants of the initial eccentricity ε_2 calculated from a sample of 20 million Pb+Pb collisions in the Monte Carlo Glauber model. We find that Eq. (14) is satisfied for central collisions, but that the left-hand side becomes larger than the right-hand side as the centrality percentile increases.

IV. MEASURING THE SKEWNESS WITH CUMULANTS

In this section we explain how to estimate the standardized skewness γ_1, defined in Eq. (6), from $v_2\{2\}$, $v_2\{4\}$ and $v_2\{6\}$. We estimate s_1 using Eq. (13). Since this result is derived from a perturbative expansion to first order in s_1, we estimate γ_1 also to first order. We, therefore, neglect small non-Gaussian contributions to $\bar{v}_2$ and σ_x: We use the Gaussian approximation, Eq. (11), which gives

$$v_2\{4\} = \bar{v}_2,$$
$$v_2\{2\}^2 - v_2\{4\}^2 = 2\sigma_x^2. \qquad (15)$$

[2] When higher-order corrections are taken into account, the asymmetry between σ_y and σ_x also produces a splitting between $v_2\{4\}$ and $v_2\{6\}$, of order $(\sigma_y^2 - \sigma_x^2)^3$; the corresponding contribution is much smaller than that of s_1 and s_2 and has opposite sign.

[3] We have not investigated the origin of the difference above 60% centrality, where the validity of the hydrodynamic description may break down and experimental data present very large error bars.

Using Eqs. (13) and (15), we obtain the following estimate of γ_1, which we denote by $\gamma_1^{\rm exp}$:

$$\gamma_1^{\rm exp} \equiv -6\sqrt{2}\, v_2\{4\}^2 \frac{v_2\{4\} - v_2\{6\}}{(v_2\{2\}^2 - v_2\{4\}^2)^{3/2}}. \qquad (16)$$

The quantities in the right-hand side can be measured experimentally and we can estimate $\gamma_1^{\rm exp}$ using the available experimental data.

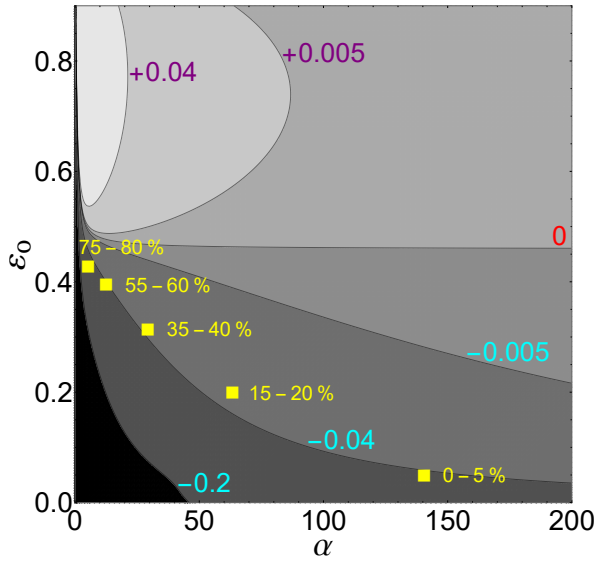

FIG. 5. (Color online) Contour plot of the difference $\gamma_1^{\rm exp} - \gamma_1$, with $\gamma_1^{\rm exp}$ defined in Eq. (16) and γ_1 defined in Eq. (6), computed by means of the Elliptic-Power distribution [12], in the (α, ε_0) parameter plane. Squares correspond to the values of α and ε_0 extracted from Monte Carlo Glauber [17] simulations of Pb+Pb collisions at 2.76 TeV, which are fitted to the Elliptic-Power distribution.

We check the accuracy of $\gamma_1^{\rm exp}$ as an estimate of γ_1 using two different methods. The first method is to compute both γ_1 and $\gamma_1^{\rm exp}$ in event-by-event hydrodynamics. $\gamma_1^{\rm exp}$ is shown as a shaded band in Fig. 2. It is in good agreement with γ_1 up to 60% centrality. Above 60% centrality, the approximation $v_2\{4\} \simeq \bar{v}_2$ breaks down, as shown by Fig. 3. Statistical errors in our hydrodynamic calculation are significant due to the limited amount of events in each centrality bin. We therefore employ a second method: We compute both γ_1 and $\gamma_1^{\rm exp}$ using the Elliptic-Power distribution [12], which is a simple analytical model for the distribution of $(\varepsilon_x, \varepsilon_y)$. The Elliptic-Power distribution has two parameters: ε_0, which approximately gives the mean eccentricity in the reaction plane, $\varepsilon_0 \simeq \langle \varepsilon_x \rangle$, and α, which is proportional to the number of participants. Fluctuations scale like $1/\sqrt{\alpha}$, therefore, the assumption of small fluctuations made in deriving Eq. (12) holds for $\alpha \gg 1$. One also expects approximations to break down in the limit $\varepsilon_0 \to 0$ (corresponding to the limiting case of the Power distribution [38]) where γ_1 vanishes by symmetry while $\gamma_1^{\rm exp}$ does not. Figure 5 indeed shows that the difference between the estimated skewness and the true skewness is large only when both α and ε_0 are small. Based on this figure, one expects the error to be a few 10^{-2} for Pb+Pb collisions, much smaller in absolute value than the value of γ_1 in Fig. 2. Therefore, Eq. (16) should provide a reasonable estimate of the standardized skewness also from experimental data.

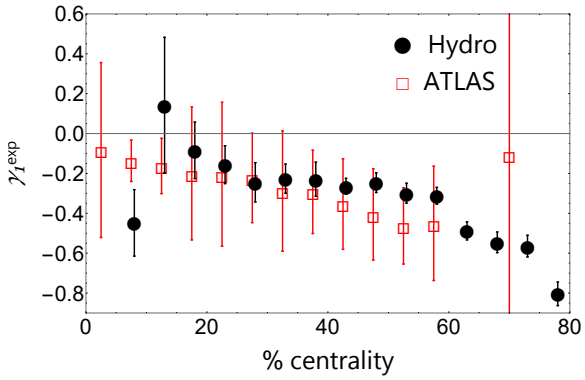

FIG. 6. (Color online) Standardized skewness of v_2 fluctuations, as defined in Eq. (16), as a function of centrality. Squares: ATLAS data. Circles: hydrodynamic calculations, corresponding to the dark shaded band in Fig. 2. Symbols have been slightly shifted horizontally for the sake of readability.

Figure 6 displays the skewness extracted from ATLAS data. It is moderate but not small, and reaches -0.5 in peripheral collisions, although with large error bars. Hydrodynamic calculations are compatible with data, as expected from Fig. 4. A finer binning in the experimental measurement above 60% centrality would help better constrain the early dynamics of the collision [39–43].

V. CONCLUSIONS

We have shown that the small splitting of higher-order cumulants of the elliptic flow from mid-central up to peripheral ultrarelativistic nucleus-nucleus collisions is mostly due to the skewness of the fluctuations of the elliptic flow in the reaction plane, v_x. We emphasize that this is a general result which does not depend on any particular model. Negative skewness is observed in Pb+Pb data, and is naturally explained in hydrodynamics: it follows from the fact that v_2 is proportional to the initial eccentricity, and that the eccentricity in the reaction plane is bounded by unity. The splitting between $v_2\{4\}$ and $v_2\{6\}$ thus provides additional evidence for the collective origin of elliptic flow. We have computed the ratio $v_2\{6\}/v_2\{4\}$ in event-by-event viscous hydrodynamics and we have shown that it is very close to the ratio $\varepsilon_2\{6\}/\varepsilon_2\{4\}$ between the cumulants of the initial eccentricity. This observable provides information about the

skewness of the initial eccentricity fluctuations, thus constraining the early dynamics of the quark-gluon plasma.

ACKNOWLEDGEMENTS

This work is supported by the European Research Council under the Advanced Investigator Grant ERC-AD-267258. JNH acknowledges the use of the Maxwell Cluster and the advanced support from the Center of Advanced Computing and Data Systems at the University of Houston to carry out the research presented here. JNH was supported by the National Science Foundation under grant no. PHY-1513864.

[1] K. H. Ackermann *et al.* [STAR Collaboration], Phys. Rev. Lett. **86**, 402 (2001) [nucl-ex/0009011].
[2] K. Aamodt *et al.* [ALICE Collaboration], Phys. Rev. Lett. **105**, 252302 (2010) [arXiv:1011.3914 [nucl-ex]].
[3] M. Luzum and P. Romatschke, Phys. Rev. C **78**, 034915 (2008) Erratum: [Phys. Rev. C **79**, 039903 (2009)] [arXiv:0804.4015 [nucl-th]].
[4] U. Heinz and R. Snellings, Ann. Rev. Nucl. Part. Sci. **63**, 123 (2013) [arXiv:1301.2826 [nucl-th]].
[5] M. Miller and R. Snellings, nucl-ex/0312008.
[6] B. Alver *et al.* [PHOBOS Collaboration], Phys. Rev. Lett. **98**, 242302 (2007) [nucl-ex/0610037].
[7] N. Borghini, P. M. Dinh and J. Y. Ollitrault, Phys. Rev. C **64**, 054901 (2001) [nucl-th/0105040].
[8] G. Aad *et al.* [ATLAS Collaboration], Eur. Phys. J. C **74**, no. 11, 3157 (2014) [arXiv:1408.4342 [hep-ex]].
[9] S. A. Voloshin, A. M. Poskanzer, A. Tang and G. Wang, Phys. Lett. B **659**, 537 (2008) [arXiv:0708.0800 [nucl-th]].
[10] L. Yan, J. Y. Ollitrault and A. M. Poskanzer, Phys. Lett. B **742**, 290 (2015) [arXiv:1408.0921 [nucl-th]].
[11] F. G. Gardim, J. Noronha-Hostler, M. Luzum and F. Grassi, Phys. Rev. C **91**, no. 3, 034902 (2015) [arXiv:1411.2574 [nucl-th]].
[12] L. Yan, J. Y. Ollitrault and A. M. Poskanzer, Phys. Rev. C **90**, no. 2, 024903 (2014) [arXiv:1405.6595 [nucl-th]].
[13] H. Grönqvist, J. P. Blaizot and J. Y. Ollitrault, arXiv:1604.07230 [nucl-th].
[14] M. Luzum, J. Phys. G **38**, 124026 (2011) [arXiv:1107.0592 [nucl-th]].
[15] H. Niemi, G. S. Denicol, H. Holopainen and P. Huovinen, Phys. Rev. C **87**, no. 5, 054901 (2013) [arXiv:1212.1008 [nucl-th]].
[16] D. Teaney and L. Yan, Phys. Rev. C **83**, 064904 (2011) [arXiv:1010.1876 [nucl-th]].
[17] B. Alver, M. Baker, C. Loizides and P. Steinberg, arXiv:0805.4411 [nucl-ex].
[18] M. L. Miller, K. Reygers, S. J. Sanders and P. Steinberg, Ann. Rev. Nucl. Part. Sci. **57**, 205 (2007) [nucl-ex/0701025].
[19] W. Broniowski, M. Rybczyński and P. Bożek, Comput. Phys. Commun. **180**, 69 (2009) [arXiv:0710.5731 [nucl-th]].
[20] J. Noronha-Hostler, L. Yan, F. G. Gardim and J. Y. Ollitrault, Phys. Rev. C **93**, no. 1, 014909 (2016) [arXiv:1511.03896 [nucl-th]].
[21] G. Policastro, D. T. Son and A. O. Starinets, Phys. Rev. Lett. **87**, 081601 (2001) [hep-th/0104066].
[22] J. Noronha-Hostler, G. S. Denicol, J. Noronha, R. P. G. Andrade and F. Grassi, Phys. Rev. C **88**, 044916 (2013) [arXiv:1305.1981 [nucl-th]].
[23] J. Noronha-Hostler, J. Noronha and F. Grassi, Phys. Rev. C **90**, no. 3, 034907 (2014) [arXiv:1406.3333 [nucl-th]].
[24] J. Noronha-Hostler, J. Noronha and M. Gyulassy, Phys. Rev. C **93**, no. 2, 024909 (2016) [arXiv:1508.02455 [nucl-th]].
[25] H. Marrochio, J. Noronha, G. S. Denicol, M. Luzum, S. Jeon and C. Gale, Phys. Rev. C **91**, no. 1, 014903 (2015) [arXiv:1307.6130 [nucl-th]].
[26] D. Teaney, Phys. Rev. C **68**, 034913 (2003) [nucl-th/0301099].
[27] J. Y. Ollitrault, Phys. Rev. D **46**, 229 (1992).
[28] J. Y. Ollitrault, nucl-ex/9711003.
[29] G. Aad *et al.* [ATLAS Collaboration], JHEP **1311**, 183 (2013) [arXiv:1305.2942 [hep-ex]].
[30] C. Adler *et al.* [STAR Collaboration], Phys. Rev. C **66**, 034904 (2002) [nucl-ex/0206001].
[31] C. Alt *et al.* [NA49 Collaboration], Phys. Rev. C **68**, 034903 (2003) [nucl-ex/0303001].
[32] S. Chatrchyan *et al.* [CMS Collaboration], Phys. Rev. C **87**, no. 1, 014902 (2013) [arXiv:1204.1409 [nucl-ex]].
[33] N. Borghini, P. M. Dinh and J. Y. Ollitrault, Phys. Rev. C **63**, 054906 (2001) [nucl-th/0007063].
[34] Z. Qiu and U. W. Heinz, Phys. Rev. C **84**, 024911 (2011) [arXiv:1104.0650 [nucl-th]].
[35] T. Hirano, P. Huovinen, K. Murase and Y. Nara, Prog. Part. Nucl. Phys. **70**, 108 (2013) [arXiv:1204.5814 [nucl-th]].
[36] P. Bożek and W. Broniowski, Phys. Rev. C **88**, no. 1, 014903 (2013) [arXiv:1304.3044 [nucl-th]].
[37] H. Niemi, K. J. Eskola and R. Paatelainen, Phys. Rev. C **93**, no. 2, 024907 (2016) [arXiv:1505.02677 [hep-ph]].
[38] L. Yan and J. Y. Ollitrault, Phys. Rev. Lett. **112**, 082301 (2014) [arXiv:1312.6555 [nucl-th]].
[39] T. Hirano, U. W. Heinz, D. Kharzeev, R. Lacey and Y. Nara, Phys. Lett. B **636**, 299 (2006) [nucl-th/0511046].
[40] R. S. Bhalerao, M. Luzum and J. Y. Ollitrault, Phys. Rev. C **84**, 034910 (2011) [arXiv:1104.4740 [nucl-th]].
[41] B. Schenke, P. Tribedy and R. Venugopalan, Phys. Rev. Lett. **108**, 252301 (2012) [arXiv:1202.6646 [nucl-th]].
[42] J. L. Albacete, A. Dumitru and C. Marquet, Int. J. Mod. Phys. A **28**, 1340010 (2013) [arXiv:1302.6433 [hep-ph]].
[43] T. Renk and H. Niemi, Phys. Rev. C **89**, no. 6, 064907 (2014) [arXiv:1401.2069 [nucl-th]].